Simulations for modeling the photothermal response of nerve tissue

Merve Turker, Serhat Tozburun

Merve Turker, Serhat Tozburun, "Simulations for modeling the photothermal response of nerve tissue," Proc. SPIE 11079, Medical Laser Applications and Laser-Tissue Interactions IX, 110791N (22 July 2019); doi: 10.1117/12.2527204

SPIE.

Event: European Conferences on Biomedical Optics, 2019, Munich, Germany

Simulations for modeling the photothermal response of nerve tissue

Merve Turker[a,b] and Serhat Tozburun*[a,b,c]

[a]Izmir Biomedicine and Genome Center, Mithatpasa St. 58/5 Balcova, TURKEY 35340; [b]Izmir International Biomedicine and Genome Institute, Dokuz Eylul University, Mithatpasa St. 58/5 Balcova, TURKEY 35340; [c]Department of Biophysics, Faculty of Medicine, Mithatpasa St. 58/5 Balcova, TURKEY 35340

ABSTRACT

Optical nerve stimulation (ONS) using infrared laser radiation is a technique developing as a potential alternative to electrical stimulation of nerve tissue. This preliminary study proposes and explores a computer simulation tool for numerically optimizing laser and surface scanning parameters including laser power and surface scanning speed to be used in laser scanning subsurface ONS. This tool consisted of three parts, including the Monte Carlo simulations for generating laser energy distribution in the tissue sample, the laser-scanning model by moving the heat source at the surface, and the thermal transfer simulations to calculate the tissue temperature. In the simulations, the laser wavelength of 1490 nm was used and the surface scan was performed on both x and y axes. In addition, the tissue model was constructed in such a way that the nerve tissue extends over the y-axis. As a result of calculations, the nerve tissue temperature map was produced as a function of laser power and surface scanning speed. According to the temperature map, the optimal laser power to reach the nerve temperature at 43 °C was estimated to be 15 mW at the scanning speeds of 1.2 mm/s in the x-axis and 1.0 mm/s in the y-axis. With further development this simulation tool may hold promise in the development of an optical stimulus device.

Keywords: Computer simulations, Monte Carlo, optical properties, optical nerve stimulation, cavernous nerves

1. INTRODUCTION

Recently, Optical Nerve Stimulation (ONS) using infrared laser radiation has been introduced as a potential alternative to electrical stimulation of the neural tissue, in vivo [1]. This technique may have significant advantages, including a non-contact stimulation method and improved spatial selectivity, for both scientific studies and clinical applications [2]. More interestingly, subsurface ONS has been demonstrated in pre-clinical model as an intermediate step towards intra-operative identification and preservation of the cavernous nerves during prostate cancer surgery [3]. In this context, we have also studied the delivery of the IR laser radiation to the nerve in continuous-wave mode [4] to investigate the operational parameters of the laser. However, with the surface scanning speed of the laser probe, these laser stimulation parameters present a large matrix of variables that needs to be optimized for consistent and reliable nerve mapping using optical stimulation of the nerve.

This novel technique of stimulation is an example of interaction of infrared light with soft tissue and is mainly mediated by a thermal process (a critical nerve temperature of ~43 °C for successful nerve activation in rat model [4]). Therefore, the optical nerve stimulation technique can be examined within the framework of the photothermal response of the biological tissue. Based on a statistical random sampling of a physical quantity, Monte Carlo simulation [5] has become the gold standard for analyzing light propagation in biological tissues. This numerical modeling technique has also been shown to be applicable to multi-layered biological tissues [6].

The aim of this study is to describe the photothermal model of the cavernous nerve that lies beneath a thin layer of fascia along the prostate surface. Using the developed photothermal model, it is intended to produce a map of the nerve tissue temperature as a function of laser power and surface scanning speed. Thermal calculations using Monte Carlo based computer simulations may be a useful tool to optimize surface scanning speed and optical stimulation parameters (i.e., laser power and nerve temperature during the stimulation) for safe and efficient laser scanning subsurface ONS.

*serhat.tozburun@ibg.edu.tr; phone 90 232 299-5101; fax 90 232 277-6353; tozburunlab.com

Medical Laser Applications and Laser-Tissue Interactions IX, edited by Lothar D. Lilge, Carsten M. Philipp, Proc. of SPIE Vol. 11079, 110791N · © 2019 SPIE · CCC code: 1605-7422/19/$21 · doi: 10.1117/12.2527204

2. METHODOLOGY

Monte Carlo modeling of laser radiation in the tissue was carried out with the multilayered approach and the source code was available in Ref. [6,7]. With this approach, the three-dimensional distribution of laser energy exposed to scattering and absorption events was modeled. The scattering coefficient and the absorption coefficient were used to define the events at each step. The step size was randomly sampled according to these optical properties of the tissue sample. The tissue sample was modeled as three-layer medium consisting of fascia, nerve and prostate. Each tissue layer forming the three-dimensional model was defined by thickness and laser wavelength-dependent optical parameters that are refractive index, scattering coefficient, absorption coefficient and anisotropy. The anisotropy factor, defined as the average cosine of the scattering angles, determined the first-degree probability distribution of the scattering angles.

In order to model time-dependent laser-induced heat transfer in the three-dimensional tissue sample, we employed the energy absorption profile computed by the Monte Carlo simulation as a heat source. These heat transfer calculations were based on Pennes' bio-heat transfer equation used for an isotropic medium with constant thermal properties. The bio-heat equation is written as: $\rho C \frac{\partial T}{\partial t} = k\nabla^2 T + Q$. Q represents the heat source of the laser irradiation (computed by the Monte Carlo simulation). k is the thermal conductivity, ρ is the density, and C is the specific heat. T is the resulting tissue temperature obtained in function of space and time by solving bio-heat equation with the time-dependent finite difference element method. According to the results of our previous study, 1490 nm was chosen as laser wavelength [3]. The diameter of the collimated Gaussian laser beam was 0.5 mm. Thermal properties, optical properties at 1490 nm, and layer thicknesses were compiled from the literature (Table 1). The physical dimensions of the modeled tissue sample were 4 mm (x, y) x 3 mm (z), where z is the depth in the tissue. This three-dimensional (r (x, y), z) tissue structure was defined as a single mesh size of 40 μm x 40 μm x 40 μm with a mesh system of 100 x 100 x 75.

To model the laser surface scanning, the distribution of the laser energy used as a heat source was shifted at a constant speed, respectively, in both axes (x-axis and y-axis). This scanning modeling method was repeated for different scanning speeds. The time step to advance the temperature solutions of the surface scan was assigned to 11 μs.

Laser induced thermal damage was assessed using a model based on the Arrhenius integral [8]: $\Omega(t) = \zeta \int_0^\tau \exp\left(\frac{E_a}{RT(t)}\right) dt$, where ζ (s^{-1}) is a frequency factor; τ (s) is the total heating time; E_a (J/mol) is an activation energy of the transformation; R (8.32 J/K mol) is the universal gas constant; and $T(t)$ is the absolute temperature of the tissue in degrees Kelvin. Numerical values of frequency factor (1.16 x 10^{55} s^{-1}) and activation energy (340 kJ/mol), corresponding to the amount of energy needed to start the transformation process, was estimated from literature previously published by Sramek et al. [9] for the retina cell.

The Monte Carlo-based model was developed in the C programming language, all other calculations and graphical analyzes were performed on the MATLAB programming platform, which provides an advanced digital computing environment. The optical and thermal properties of the tissue model were assumed to be independent of temperature changes. To accurately model the distribution of absorbed radiation in the tissue layers, the required unit-weighted total photon number, depending on the spatial resolution in the simulation, was used as one million. The initial tissue temperature was set to 37 °C.

Table 1: Optical properties at 1490 nm, thermal properties, and layer thicknesses.

Optical Properties and Thermal Properties			
	Fascia	Nerve (white matter)	Prostate
Absorption coefficient, cm^{-1}	7 [10]	28 [12]	53.9 [13,16]
Reduced scattering coefficient, cm^{-1}	15 [10]	5.9 [13]	5.61 [13]
Anisotropy factor	0.8 [10]	0.9 [14]	0.9 [14]
Refractive index	1.318 [11]	1.467 [15]	1.4 [15]
Layer thickness, cm	0.011	0.03	0.259
Thermal conductivity, W/m°C	0.47 [17]	0.503 [18]	0.5 [19]
Specific heat, J/kg°C	3.2 [17]	3.6 [18]	3.78 [19]
Density, kg/m^3	$1.085e^6$ [17]	$1.027e^6$ [18]	$1.06e^6$ [19]

3. RESULTS

Figure 1 shows a representation model of the tissue sample containing the fascia (blue), nerve (white color) and prostate (red color) layers. A 300 μm diameter nerve was placed along the y-axis below a thin fascia layer (110 μm) and was centered on both axes. The total tissue thickness was 3 mm. Figure 2 shows an example of a solution of the heat transfer

equation that defines the temperature history of the tissue as a function of depth and lateral positions. In this simulation, the scan speed was set to 0.6 mm/s in x-axis and 1.0 mm/s in y-axis, respectively. En-face and cross-section transient temperature profiles were chosen for each end of the scan. The scanning time was calculated to be 2.0 s for the x-axis and 3.5 s for the y-axis. The representative temperature profiles were obtained for the laser power of 20 mW. During the surface scan, the maximum nerve temperature was calculated to be 45.8 °C.

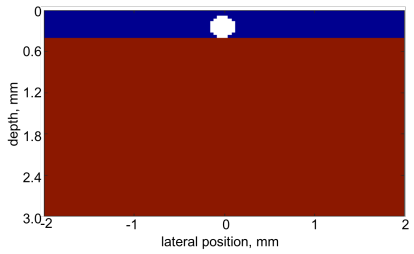

Figure 1. A 2D (x-axis and depth) representation of the tissue model that contains the fascia (blue), nerve (white color) and prostate (red color) layers. The diameter of the nerve is 300 µm and the nerve extends along the y-axis.

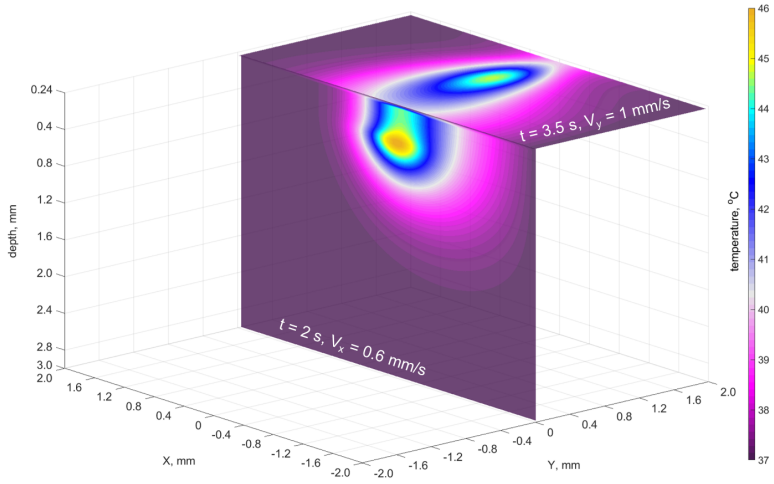

Figure 2. En face and cross-sectional frames of transient tissue temperature profile.

The similar simulations were repeated for a power range of 0.5 - 100 mW at different scan speeds to map the maximum nerve temperature as the surface scanning speeds and the laser power matrix (Figure 3). To facilitate simulations at this level of study, the surface scanning speed was changed from 0.4 to 1.2 mm/s for the x-axis, and from 0.5 to 2.0 mm/s for the y-axis. In addition, single-line scanning was simulated on both axes instead of field scan. A theoretical damage threshold was calculated for each laser power level at different speeds using the Arrhenius integral model. The critical temperature was calculated to be 48.2 °C for the frequency factor of 1.16 x 10^{55} s^{-1} and activation energy of 340 kJ/mol [9]. The thermal damage threshold level is highlighted as a white solid line on the map. Not surprisingly, the slow scanning speed and high laser power produced very high nerve tissue temperature which is beyond the thermal damage threshold levels. A critical nerve temperature of ~43 °C for successful nerve activation by using ONS was reported in the literature [4]. We estimated that the optimal laser power to reach the nerve temperature at >43 °C was about 15 mW at the scanning speeds of 1.2 mm/s in the x-axis and 1.0 mm/s in the y-axis. The total surface scan time was 2.5 s.

4. DISCUSSION

The optical stimulation of nerves is a new developing technique. In some complex clinical applications such as neural mapping, the laser and surface scanning parameters that need to be optimized can create a large matrix of variables. Conditions such as mapping the Cavernous nerves in the human prostate that extend below the fascia layer varying from 100 - 300 µm in diameter [20] can make the matrix even more complex. This preliminary study investigates a simulation

tool that uses Monte-Carlo methods to simulate photothermal manipulation of the Cavernous nerve underlying a thin fascia layer along the prostate surface.

There are a few points to discuss briefly for our simulation studies. First, the values of the absorption and scattering coefficients are assumed to be constant over time. Second, it may also be necessary to investigate more complex tissue structure involving blood vessels to analyze heat dissipation. Finally, the laser surface scan simulation can be applied to the field at several speeds instead of applying to the lines on both axes to expand the variable matrix of the surface scanning subsurface optical nerve stimulation (ONS).

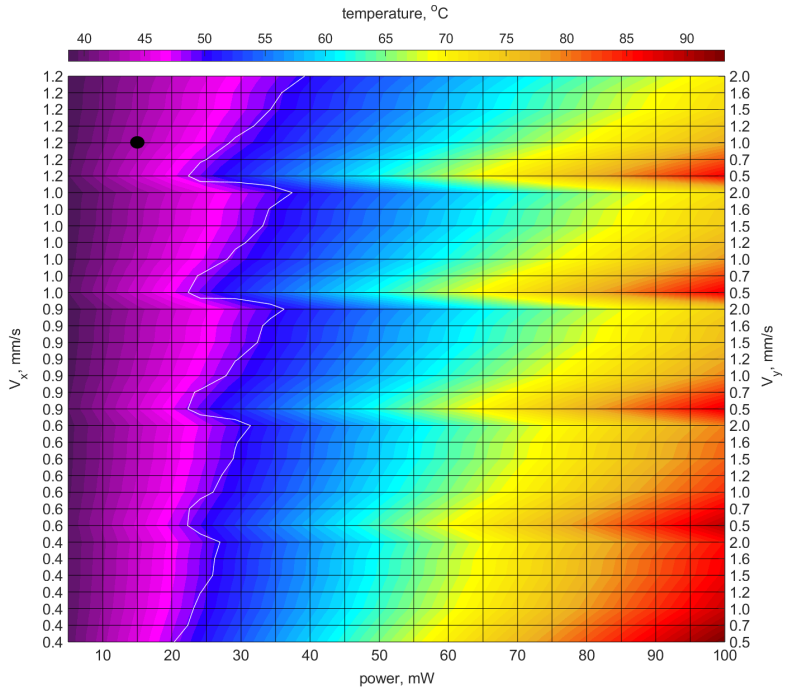

Figure 3. The maximum nerve temperature map reached during surface scanning as a function of laser power and surface scanning speed. The black spot marks the optimum point at which the nerve reaches 43 °C in terms of high surface scanning speed and low laser power. The white solid line indicates the thermal damage threshold caused by the laser radiation at a critical temperature of 48.2 °C.

5. CONCLUSIONS

This study has demonstrated a computer simulation tool as a complementary component to future pre-clinical and clinical surface scanning subsurface optical nerve stimulation studies. This simulation tool with further development may hold promise in the development of an optical stimulus device that provides intraoperative mapping of the neural tissue.

ACKNOWLEDGMENTS

This work was supported partially by TÜBITAK grant No [117E985] and the European Union's Horizon 2020 research and innovation programme under the Marie Skłodowska-Curie grant agreement No [835907]. Merve Turker was supported by a Turkish Council of Higher Education 100/2000 doctoral scholarship.

REFERENCES

[1] Wells, J., Kao, C., Mariappan, K., Albea, J., Jansen, E. D., Konrad, P. and Mahadevan-Jansen, A., "Optical stimulation of neural tissue in vivo," Opt. Lett. 30(5), 504-506 (2005).

[2] Wells, J., Kao, C., Jansen, E. D., Konrad, P. and Mahadevan-Jansen, A., "Application of infrared light for in vivo neural stimulation," J. Biomed. Opt. 10(6), 1-11 (2005).

[3] Tozburun, S., Lagoda, G. A., Burnett, A. L. and Fried, N. M., "Continuous-wave infrared subsurface optical stimulation of the rat prostate cavernous nerves using a 1490 nm diode laser," Urology 82(4), 969-973 (2013).
[4] Tozburun S., Hutchens, T. C., McClain, M. A., Lagoda, G. A., Burnett, A. L. and Fried, N. M., "Temperature controlled optical stimulation of the rat prostate cavernous nerves," J. Biomed. Opt. 18(6), 067001 (2013).
[5] Wilson, B. C. and Adam, G., "A Monte Carlo model for the absorption and flux distributions of light in tissue," Med. Phys. 10(6), 824-830 (1983).
[6] Wang, L. H., Jacques, S. L. and Zheng, Z., "MCML - Monte-Carlo modeling of light transport in multilayered tissues," Comput. Methods Programs Biomed. 47(2), 131-146 (1995).
[7] Jacques, S. L. and Li, T., " Monte Carlo simulations of light transport in 3D heterogenous tissues (mcxyz.c)," Available at https://omlc.org/software/mc/mcxyz/index.html, Version June 1, 2017.
[8] Henriques, F. C. and Moritz, A. R., "Studies of Thermal Injury .1. The Conduction of Heat to and through Skin and the Temperatures Attained Therein – a Theoretical and an Experimental Investigation," Am. J. Pathol 23(4), 531-549 (1947).
[9] Sramek, C., Paulus, Y., Nomoto, H., Huie, P., Brown, J. and Planker, D., "Dynamics of retinal photocoagulation and rupture," J. Biomed. Opt. 14(3), 034007 (2009).
[10] Kozintseva, M. D., Bashkatov, A. N., Kochubey, V. I., Genina, E. A., Gorodkov, S. Y., Morozov, D. A. and Tuchin, V. V., "Optical properties of parietal peritoneum in the spectral range 350-2500 nm," Proc. SPIE 9031, 90310E (2014).
[11] Hale, G. M. and Querry, M. R., "Optical constants of water in the 200nm to 200um wavelength region," Appl. Opt. 12(3), 555-563 (1973).
[12] Dirnagl, U., Villringer, A. and Einhaupl, K. M., [Optical Imaging of Brain Function and Metabolism], Springer Science+Business Media, New York, 53 (1993).
[13] Jacques, S. L., "Optical properties of biological tissues: a review," Phys. Med. Biol. 58, 37-61 (2013).
[14] Niemz, M. H., [Laser-Tissue Interactions: Fundamentals and Applications, 3rd Enlarged Edition], Springer, Berlin Heidelberg, 23 (2007).
[15] Pawley, J., [Handbook of Biological Confocal Microscopy, 3rd Edition], Springer Science+Business Media, New York, 377 (2006).
[16] Sordillo, A. L., Pu, Y., Pratavieira, S., Budansky, Y. and Alfano, R. R., "Deep optical imaging of tissue using the second and third near-infrared spectral windows," J. Biomed. Opt. 19(5), 056004 (2014).
[17] Hardy, L. A., Chang, C.-H., Myers, E. M., Kennelly, M. J. and Fried, N. M., "Computer simulations of thermal tissue remodeling during transvaginal and transurethral laser treatment of female stress urinary incontinence," Lasers Surg. Med. 49(2), 198-205 (2017).
[18] Collins, C. M., Smith, M. B. and Turner, R., "Model of local temperature changes in brain upon functional activation," J. Appl. Physiol. 97, 2051-2055 (2004).
[19] Manuchehrabadi, N. and Zhu, L., "Development of a computational simulation tool to design a protocol for treating prostate tumours using transurethral laser photothermal therapy," Int. J. Hyperthermia 30(6), 349-361 (2014).
[20] Takenaka, A., Murakami, G., Matsubara, A., Han, S. H. and Fujisawa, M., "Variation in course of cavernous nerve with special reference to details of topographic relationships near prostatic apex: histologic study in male cadavers," Urology 65, 136-142 (2005).